

# Morphological barrier island changes and recovery of dunes after Hurricane Dennis, St. George Island, Florida

A.M. Priestas<sup>\*</sup>, S. Fagherazzi

Department of Earth Sciences, Boston University, 675 Commonwealth Ave, Boston Massachusetts 02215, USA

## ARTICLE INFO

### Article history:

Received 4 March 2009

Received in revised form 30 August 2009

Accepted 1 September 2009

Available online 17 September 2009

### Keywords:

Dune recovery

LiDAR

Overwash

Hurricane Dennis

Barrier island

## ABSTRACT

During the summer of 2005, Hurricane Dennis overwashed the eastern portion of St. George Island, part of the northwest barrier island chain located along the Florida Panhandle. In this paper, LiDAR-based morphological changes of the barrier island are analyzed, along with the short-term post-storm recovery of secondary dunes. Results show that overwash from the storm surge removed nearly the entire foredune complex, and the initial breaching probably occurred where the complex was either low or discontinuous; in these locations, beach widening was less. In contrast, approximately 10 m of beach widening occurred where foredunes were higher and continuous, implying that more sediment was available for seaward transport during storm conditions. The secondary dunes recovered at an average linear rate of 3–4 cm per month in the presence of vegetation, although monthly averages varied from  $-1.5$  to  $1.4$  m<sup>3</sup>/m and total volume changes varied from  $-17.9$  to  $16.4$  m<sup>3</sup>/m for the duration of the study. Furthermore, vegetation deterred dune migration, thus favoring dune growth and reducing erosion due to wind. In contrast, the absence of vegetation inhibited dune growth. Insignificant changes in elevation occurred in areas of storm debris or lag deposit. Finally, distributions of topographic gradients and curvature calculated numerically from pre- and post-storm LiDAR data are introduced as a potential tool in determining the relative post-storm recovery of the dune field.

© 2009 Elsevier B.V. All rights reserved.

## 1. Introduction

Dennis made landfall as a category 3 hurricane on July 10th, 2005 near Pensacola, Florida less than 1 year after Hurricane Ivan (also a category 3) struck the panhandle approximately 80 km west of Dennis. Sustained winds from Dennis at landfall were reported at 51–53 m/s (115–120 mph) with the storm center moving on a northwesterly track. The storm surge at St. George Island (280 km east of the eyewall) was reported to be 2.5 m above mean lower low water at the time of Dennis' landfall. Storm-track direction and offshore bathymetry may have resulted in a higher storm surge at St. George Island compared to other reaches of the coast closer to the eyewall (e.g. the storm surge at Panama City Beach, ~75 km east of the eyewall, was about 1.7 m).

Washover deposits as a result of the high storm surge translated large amounts of sediment to the back-barrier, and where St. George Island is narrow those deposits extended to the waters of St. George Sound. The impact of overwash was apparent, as trees were inundated by sediment, the back-barrier was denuded of vegetation and rendered featureless, and the roadway destroyed and displaced by tens of meters.

The foredune complex, while protective, can be quite vulnerable to storm surge and wave attack, especially along sections that are at lower elevation or discontinuous. Sallenger (2000) stated that a

storm's ability to overwash a barrier depends on storm-surge elevation, wave height, storm-wave set-up and swash run-up, and foredune height. Additionally, Morton and Sallenger (2003), and Wang et al. (2006) noted that overwash can also occur in cases where the storm tide is lower than foredune height due to wave run-up and dune scarping. Other factors that increase dune survival are vegetation density, presence of woody vegetation, dune field continuity, dune field width, and barrier island width (Claudino-Sales et al., 2008). In the present study, we observe a qualitative correlation between pre-storm foredune height and sediment volume change.

The resulting washover deposit may sometimes conserve the mass of the barrier island (Stone et al., 2004); although Donnelly et al. (2006) noted that from a coastal management perspective washover sediment is accounted for as a sink term in the littoral sediment budget. The breaching or lowering of the foredune increases the risk of overwash causing damage to infrastructure and habitats by flooding, scouring, and wave attack. Low-elevation barriers are especially susceptible to such storm activity from both hurricanes (Stone et al., 2005) and cold-front systems (Dingler and Reiss, 1990).

Digital elevation models (DEMs) from Light Detection and Ranging (LiDAR) data provide the means to investigate the redistribution of sediment volumetrically and to note morphological changes that occurred within a selected portion of St. George Island State Park.

The purpose of this study is three-fold: 1) describe the post-storm morphological changes and calculate the redistribution of sediment from LiDAR datasets, 2) introduce a simple numerical technique to

<sup>\*</sup> Corresponding author. Tel.: +1 617 353 4086; fax: +1 617 353 3290.

E-mail addresses: [priestas@bu.edu](mailto:priestas@bu.edu) (A.M. Priestas), [sergio@bu.edu](mailto:sergio@bu.edu) (S. Fagherazzi).

evaluate the future relative dune recovery state using LiDAR-derived distributions of topographic gradients and curvatures, and 3) monitor the short-term recovery of secondary dunes and the effect of vegetation on dune evolution.

The use of LiDAR to investigate coastal geomorphology has become common among geomorphologists, engineers, and coastal management personnel (van Der Wal, 1996; Irish and White, 1998; Sallenger et al., 1999; Andrews et al., 2002; Saye et al., 2005; Sallenger et al., 2006; Robertson et al., 2007), as increases in vertical accuracy, spatial resolution, and post-processing allows for such investigations of coastal environments at low cost.

Despite its high spatial resolution (~1.5 m in our study site) LiDAR altimetry cannot fully capture the evolution of small morphological features like incipient dunes establishing on flat surfaces or the distribution and dynamics of short vegetation. Moreover, LiDAR datasets are expensive and seldom collected; as a result they cannot be used to track dune recovery on a month to annual timescale. For these reasons we integrate the LiDAR datasets with high resolution (sub-meter) surveys along five transects. The surveys include important information on vegetation distribution and its effects on dune evolution.

Vegetation plays a critical role for both dune stability and recovery after storms and hurricanes. Stallins (2001) showed that common dune building plants, such as high growing *Uniola paniculata* (sea oats), are effective in trapping sediment and accelerating dune growth. The ability

of vegetation to trap sediment is based on decreases in wind velocities below the canopy surface as a result of increased surface roughness (Buckley, 1987; Hesp, 1989; Hesp et al., 2005). In fact, Buckley (1987) showed experimentally that the sand transport rate decreased to 16% and 22% of the initial transport rate using  $10 \text{ ms}^{-1}$  and  $15 \text{ ms}^{-1}$  wind velocities, respectively, and using 17% plant cover 10 cm high and 12 cm across. Similarly, Arens (1996) showed that vegetation cover of 30% can effectively stop aeolian transport.

Sea oats typify the vegetation among dunes of the study area, and are especially adapted to many physical stresses such as wind, storms, and salt spray making them ideally suited for coastal environments (Woodhouse et al., 1968). Snyder and Boss (2002) noted that sea oats recovered rapidly from dispersed colonies after storm surges from hurricanes Opal and Erin scoured many areas of Santa Rosa Island, Florida in 1995.

## 2. Study site

St. George Island (SGI) State Park occupies the easternmost 14 km of St. George Island, one of the easternmost segments of the northwest Florida barrier island chain (Fig. 1). The barrier is wave-dominated and microtidal with a mean tidal range of 34 cm and mean diurnal range of 49 cm (NOAA tide station 8728690). Sediment composition is comprised of fine to medium-fine >99% quartz sand, although there is

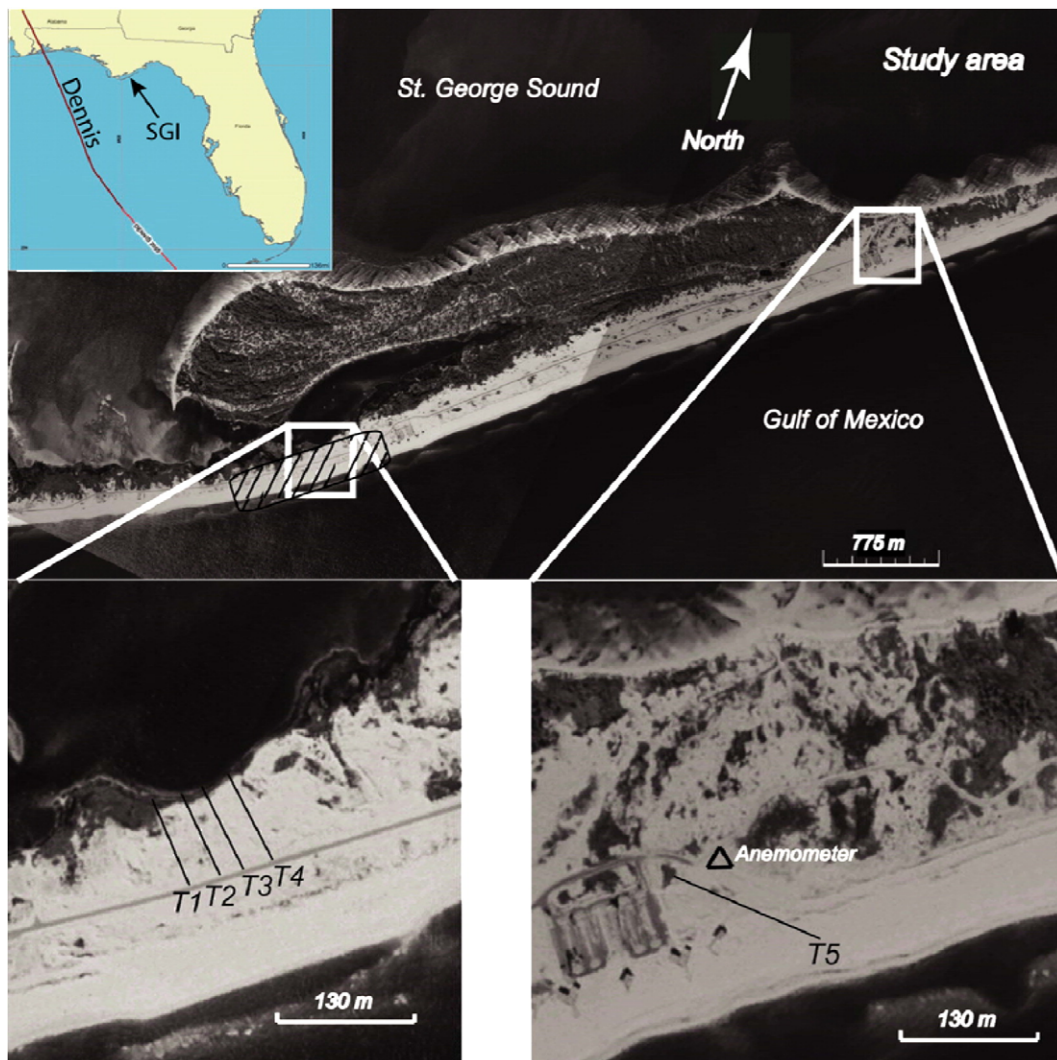


**Fig. 1.** USGS orthophotos (1999) of St. George Island State Park and corresponding study sites where profile measurements were taken. Study site 1 (A) contains four transects each about 100 m in length, while study site 2 (B) shows the locations of transect 5 and the anemometer. The striped area shows the approximate location of LiDAR data used in this study.

now a considerable amount of asphalt and shell detritus from the storm surge which formed a lag deposit in many areas of the island.

Hourly averaged data collected from NOAA weather station APCF1 in Apalachicola, Florida spanning 1 year between July 1st, 2004 to July 1st, 2005 revealed that winds exceeding 10 m/s were mostly from the ENE and occurred at least 2% of the specified time, while more moderate winds (but still capable of moving sediment) occurred at least 20% of the time and were more northerly. In situ measurements of wind direction frequencies from June, 2006 to December, 2006 were nearly evenly distributed with the strongest winds measured from the north, east, and south directions (Fig. 2). Of these, the dominant winds tended to be from the east and north. These findings are consistent with the average historical wind data reported by the Florida State University Beaches and Shores Research Center (1983).

The study site was largely chosen because it closely resembles a pristine system with minimal infrastructure and anthropogenic

impact or modifications to the landscape. Other areas of the park were subject to artificial dune building along the roadside which may have affected the sediment transport dynamics across the study areas.

Similar studies on the impact of hurricanes on barrier islands have been carried out in recent years by Stone et al. (2005) along the Northern Gulf of Mexico, by Wang et al. (2006) along the Panhandle Florida coast from Fort Walton Beach to St. George Island, and by Houser et al. (2008b) and Houser and Hamilton (2009) on Santa Rosa Island, Florida. In particular, Wang et al. (2006) measured beach and dune erosion after hurricane Ivan in St. George Island, determining an elevation loss between 0.3 to 0.7 m over a 40 m-wide stretch of back-beach. Contrary to hurricane Dennis, no overwash was detected during Ivan, but extensive scarping of the foredunes with wave erosion reaching 2 m above mean sea level. Beach and berm recovery started just after hurricane Ivan and was almost completed after 90 days (Wang et al., 2006).

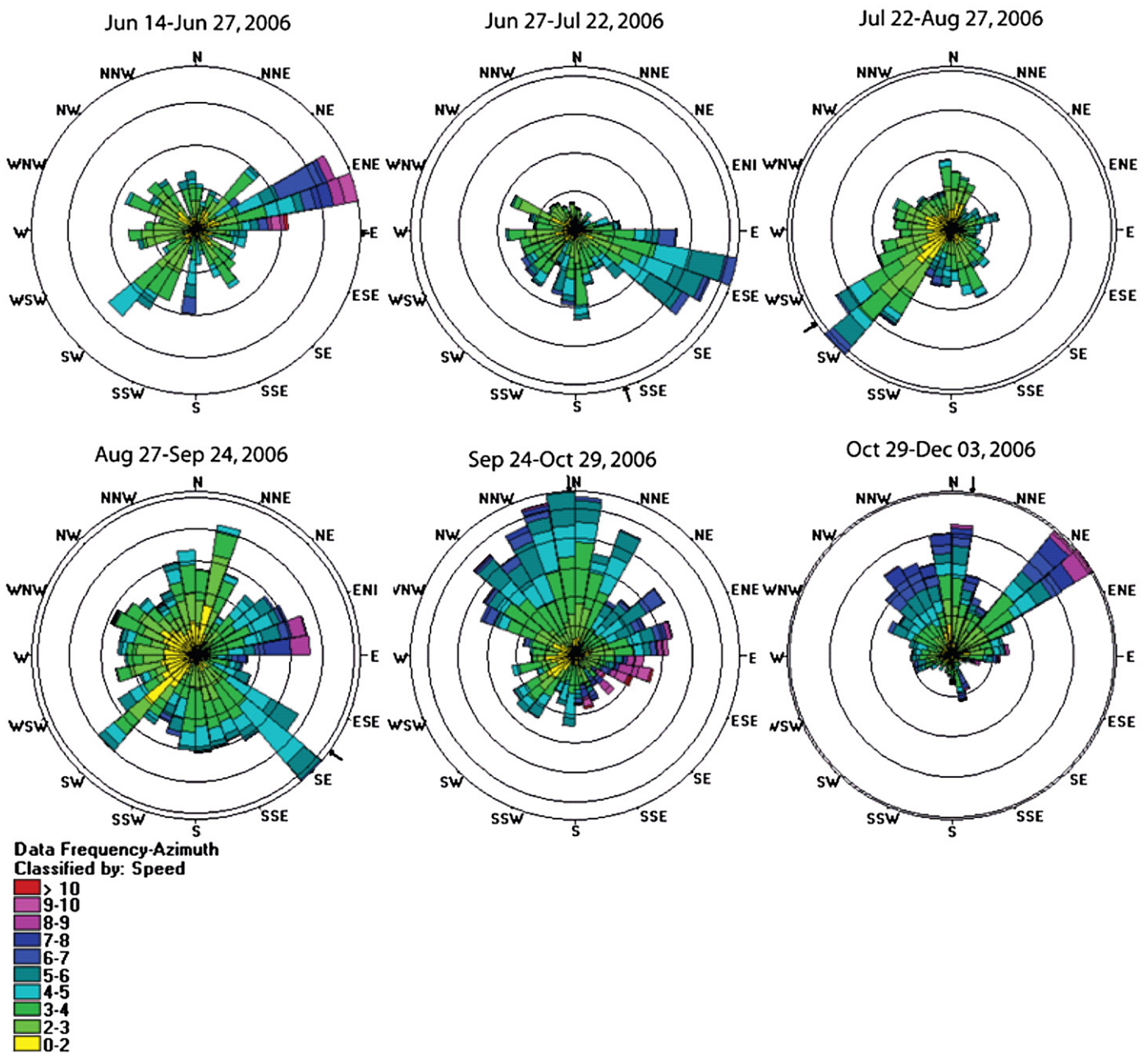


Fig. 2. Rose diagrams for SGI wind data from June 14th–December 3rd 2006, classified by wind speed in m/s.

**3. Methods**

**3.1. LiDAR data and DEM analysis**

Post-storm morphological changes are described by using LiDAR data, which utilizes an airborne-mounted laser in parallel with a kinematic differential GPS to map the ground surface by measuring the time delay between an object and the aircraft (Brock et al., 2002). The raw data is then post-processed to remove vegetation and structures, corresponding to a bare-earth representation of the surface. The vertical accuracy of the data is approximately 0.15 m. The pre-Dennis LiDAR data was collected by the University of Florida’s Airborne Laser Swath Mapping (ALSM) system in May 2004, while post-Dennis LiDAR data was collected between July 8th and July 31st, 2005 by the Joint Airborne LiDAR Bathymetry Center of Expertise (JALBTCX). For a summary of the basic principles and processing of airborne-based LiDAR data see Brock et al. (2002). Pre- and post-Dennis topography can be visualized using digital elevation models (DEMs), which are user defined grid data representing terrain elevations. The DEMs in this study were created by taking the post-processed *x*, *y*, *z* data and gridding them into a 1.5 × 1.5 m (5 × 5 ft) cell matrix using Transform® software, which were subsequently filled using a linear interpolation algorithm and uploaded into Matlab™ for analysis. The spatial extent of LiDAR coverage used in our analysis encompasses a 200 × 2000 m area indicated by the swathed pattern in Fig. 1A.

The relative dune recovery state, or system recovery state, can be represented by a distribution of topographic gradients representing surfaces of either flat (zero value) or undulating topography. For each cell of a DEM, the gradient, *G*, was calculated using a 3-point central difference scheme for pre- and post-storm data, while the curvature, *C*, was calculated using a 5-point stencil using the numerical formulae:

$$G_{R,C} = \frac{\partial f}{\partial x} = \sum \frac{(f_{R,C+1} - f_{R,C-1})}{2\Delta x} \tag{1}$$

and

$$C_{R,C} = \frac{\partial^2 f}{\partial x^2} = \sum \frac{(f_{R+1,C} + f_{R-1,C} + f_{R,C+1} + f_{R,C-1} - 4f_{R,C})}{\Delta x^2} \tag{2}$$

where *R* and *C* are row and column values, respectively,  $\Delta x$  is the cell width (in this case 1.5 m), and *f* is the value of the elevation for a given cell. The gradient for each cell is calculated across the shore-perpendicular (*G<sub>v</sub>*), shore-parallel (*G<sub>H</sub>*), and left–right oblique (*G<sub>L</sub>*, *G<sub>R</sub>*) directions, which are then binned at 0.005 (unitless) intervals and plotted as frequency distributions to be compared before and after hurricane Dennis. Greater than 95% of the gradient values fall between –0.2 and +0.2 and are plotted as such.

To investigate changes in sediment redistribution and morphology, pre- and post-storm DEMs were subtracted from one another and visualized as an elevation change map (ECM). The DEMs were rotated in Matlab™ 30° using a trigonometric transform function in order to take the cross-shore numerical integration of the DEMs, using the trapezoidal method, allowing for quantitative estimation of post-storm volume changes. We estimated post-storm volume changes by applying a cross-shore numerical integration using the trapezoidal method:

$$V = \int_a^b f(x) dx = \sum_a^b (x_2 - x_1) \frac{f(x_1) + f(x_2)}{2} \tag{3}$$

where *V* is the total volume, *a* and *b* are the control points, *x*<sub>1</sub> and *x*<sub>2</sub> are points between each measurement, and *f*(*x*<sub>1</sub>) and *f*(*x*<sub>2</sub>) are the corresponding values of dune height. The result was normalized to the cell width of 1.5 m for each column of the ECM matrix and the net volume change (reported in m<sup>3</sup>/m) was calculated by integrating the difference between the earliest and last profile for a given transect. The volume was then divided by the shoreline length to give the average volume change per meter length of beach.

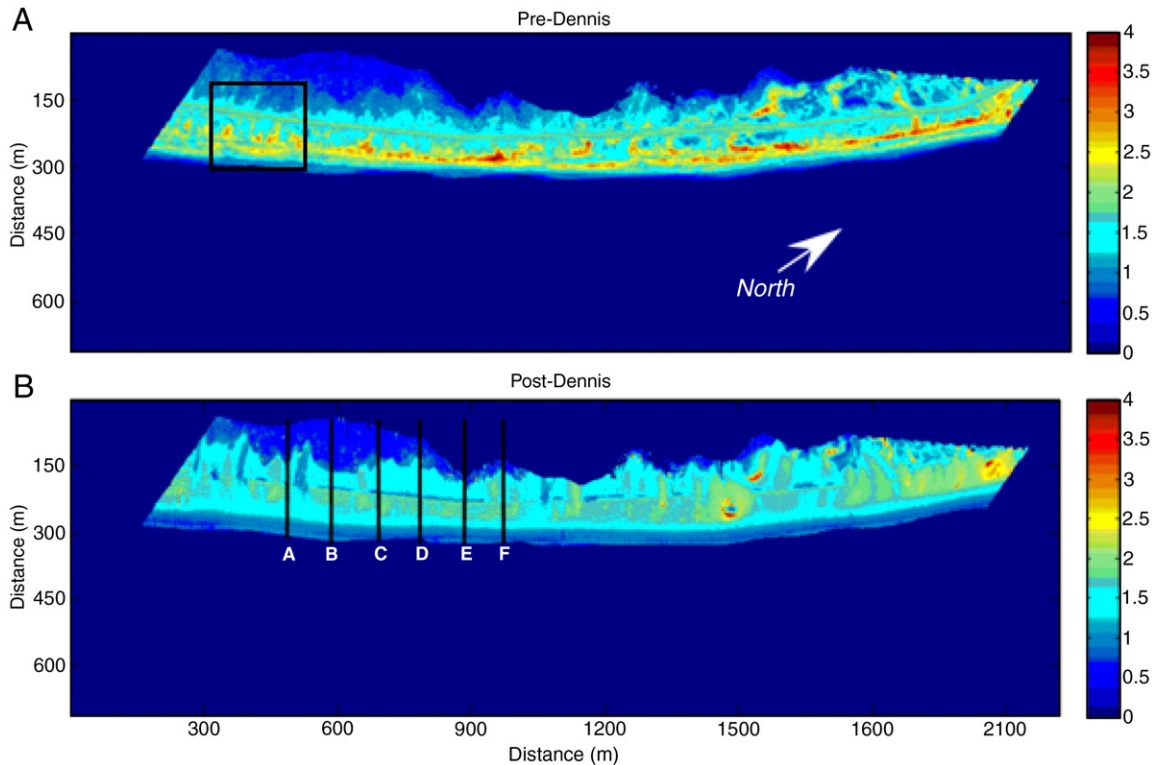


**Fig. 3.** Digital elevation models (DEMs) of ~2 km section of SGI State Park pre-storm (A; May 2004) and post-storm (B; July 2005). Before and after profiles extracted from the DEMs are shown as the black lines A–F (see Fig. 5). Color bar in meters of elevation. Distances are relative.

### 3.2. Wind data

To observe the response of dunes to changing wind climate, wind data was collected from June 18th to December 3rd 2006 by use of a wind-cup anemometer attached to a data-logging device; it should be noted, however, that premature battery failure did not permit full overlap with transect data by about 1 month. The instrument was attached to a 4 m anchored tripod and was deployed about 200 m landward of the shoreline. The sampling frequency was 1 Hz, and the maximum and average wind speeds along with average wind direction were logged every 10 min. The direction of the instrument sensor was oriented with a Brunton compass, adjusted for magnetic declination of the area.

Analysis of wind direction frequencies was performed using the freeware Georient™. The wind roses are classified by mean wind speed, and each ring in a sector represents a percentage of the data. The arrow on the plot indicates the resultant mean direction and includes the 95% confidence interval (shown by the arc). Wind direction is reported in the direction the wind is coming from.

### 3.3. Survey of secondary dunes recovery

Time-series surveys of the back-barrier were taken to investigate the short-term recovery of secondary dunes. Five transects were taken using a Topcon™ surveying total station. For each transect, a graduated line was extended between two control points with each graduation on the line measuring approximately 0.5 m. Four transects (T1–T4) were approximately 100 m in length and extended from the road to the bay (Fig. 1B). The fifth transect (T5) was approximately 170 m in length and extended from the road to the beach (Fig. 1C). The Topcon™ total station is capable of measuring a position accurately to within 5 mm at 100 m distance. Small (mm-scale) errors can be introduced by slight variations in instrument set-up and deviations from vertical with respect to the prism rod but are considered insignificant.

For each transect, the profiles were plotted relative to the first control point and were not tied to any datum. The top of the sediment surface was marked on each of the control point stakes to track erosion or deposition to allow for corrections to the profiles; as it were, no net erosion or deposition occurred to any significant degree at the control point for each transect.

To quantify dune recovery, time-series profiles were plotted and sediment volume changes between time intervals were estimated using the trapezoidal method of numerical integration (Eq. (1)). Careful consideration was given when interpreting profile changes since translations in the dunes may plot as large changes in profile height, but it is not necessarily related to dune accretion. Therefore, volume changes can only be significant across the entire profile and not for any particular point within the profile.

Surveying began October 2005 and ended February 2007. Four profiles were obtained for transect 1 (October 2005–February 2007), four profiles for transects 2 and 3 (October 2005–October 2006), five profiles for transect 4 (October 2005–February 2007), and eight profiles for transect 5 (May 2006–February 2007). Data collection for transects 1–4 were halted for a six month duration (April 2006–September 2006) due to protected nesting birds, affecting the temporal resolution of profile changes in conjunction with measured wind events.

## 4. Results

### 4.1. Topographic and sediment volume changes

Fig. 3 shows the pre- and post-storm topography derived from LiDAR data. In Fig. 3A, the foredune complex, reaching between 2.5–4 m, is not continuous but instead has many breaches and low-elevation points along its front, most noticeably along the first 400 m

of the section. These areas are vulnerable to storm surges and have probably acted as conduits where flooding water is concentrated to form washover throats. The post-storm topography in Fig. 3B reveals the extent of overwash that occurred throughout the park. Nearly the entire foredune complex was removed, as sediment was displaced landward as a series of washover fans (or a washover apron in the western half). Foredunes in the eastern end of the section were more continuous and were approximately 60 cm higher in elevation, thus having fewer possible overwash throats than the western section. On average, washover deposits were approximately 20 m wide at 60 m spacing. The spacing and morphologic structure of the washover fans and throats generally coincides with pre-storm topography shown in Fig. 4.

Pre- and post-storm profiles were extracted from the DEM's across transects indicated by the black lines in Fig. 3B, and are presented in Fig. 5A–F. In addition to the beach widening, a post-storm ridge and runnel system developed, which is typical and evident in each profile. Each profile shows the removal of the foredune complex and the

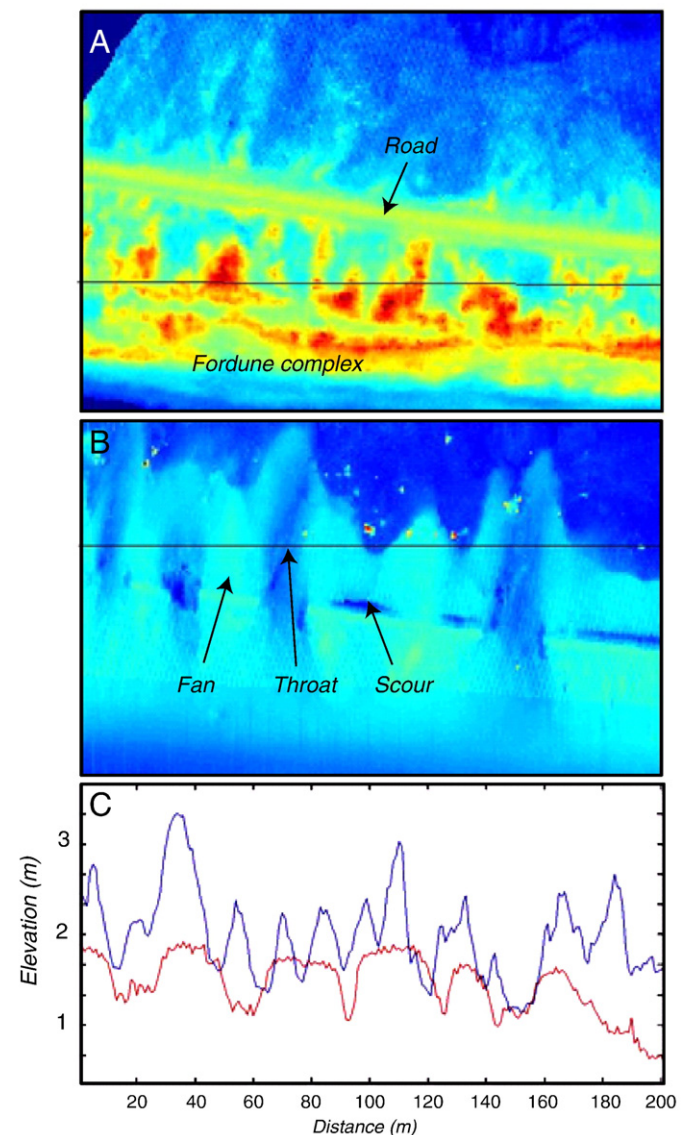
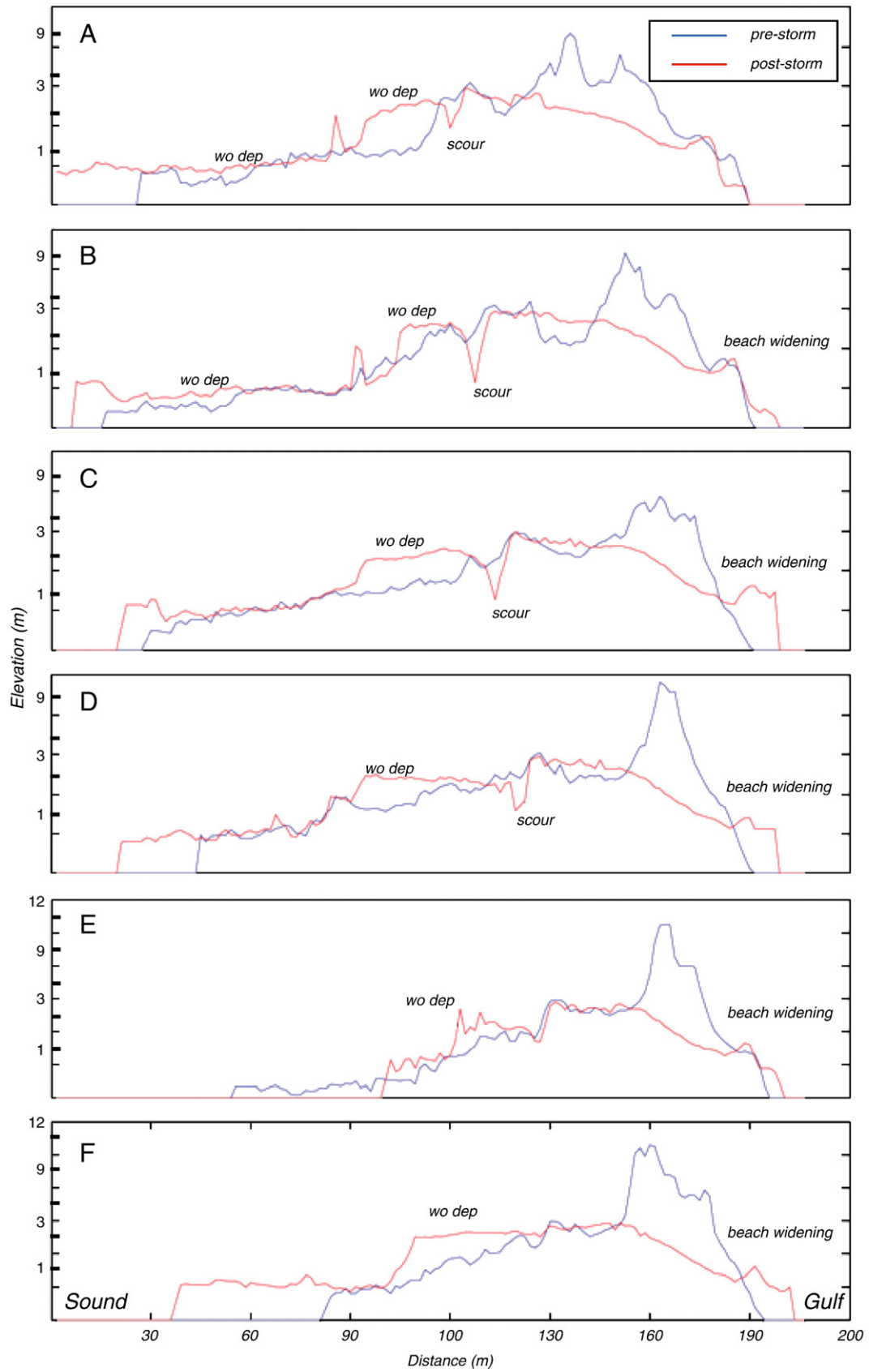


Fig. 4. Extracted profiles (C) shown by the black line across (A) pre-storm topography and (B) post-storm washover fan topography. The two profiles are plotted in (C) and show the general association between the pre-storm profile (blue) and post-storm profile (red). This portion of the DEM is shown by the black box in Fig. 3A.



**Fig. 5.** Extracted DEM profiles (black lines A–F in Fig. 3B.). Pre-storm profiles are shown in blue, while post-storm are in red. Each set of profiles shows the removal of the foredune and subsequent landward washover deposits. Beach widening occurred to various degrees but was noted that widening was more prevalent in the eastern side of the study area.

deposition of a washover deposit. The washover deposits tend to terminate abruptly landward, seen by the sharper gradient, suggesting that washover penetration may not have reached the sound in this area. The minimum thickness of the washover deposits is of the order of 50–60 cm not accounting for erosion of the pre-storm surface, similar to that of other overwashed barriers (Wang et al., 2006). It is interesting to note that despite the removal of the foredune, some sections of the profile in

Fig. 5E maintained their original morphology between the original foredune and the washover deposit. Perhaps more sediment was moved offshore, or laterally. The large scour marks in each of the profiles denotes the road surface, most of which was washed away.

The elevation change map (ECM) clearly shows the washover deposits and overall sediment redistribution (Fig. 6A). Blue colors (or light areas) in the ECM indicate erosion whereas red colors (or dark

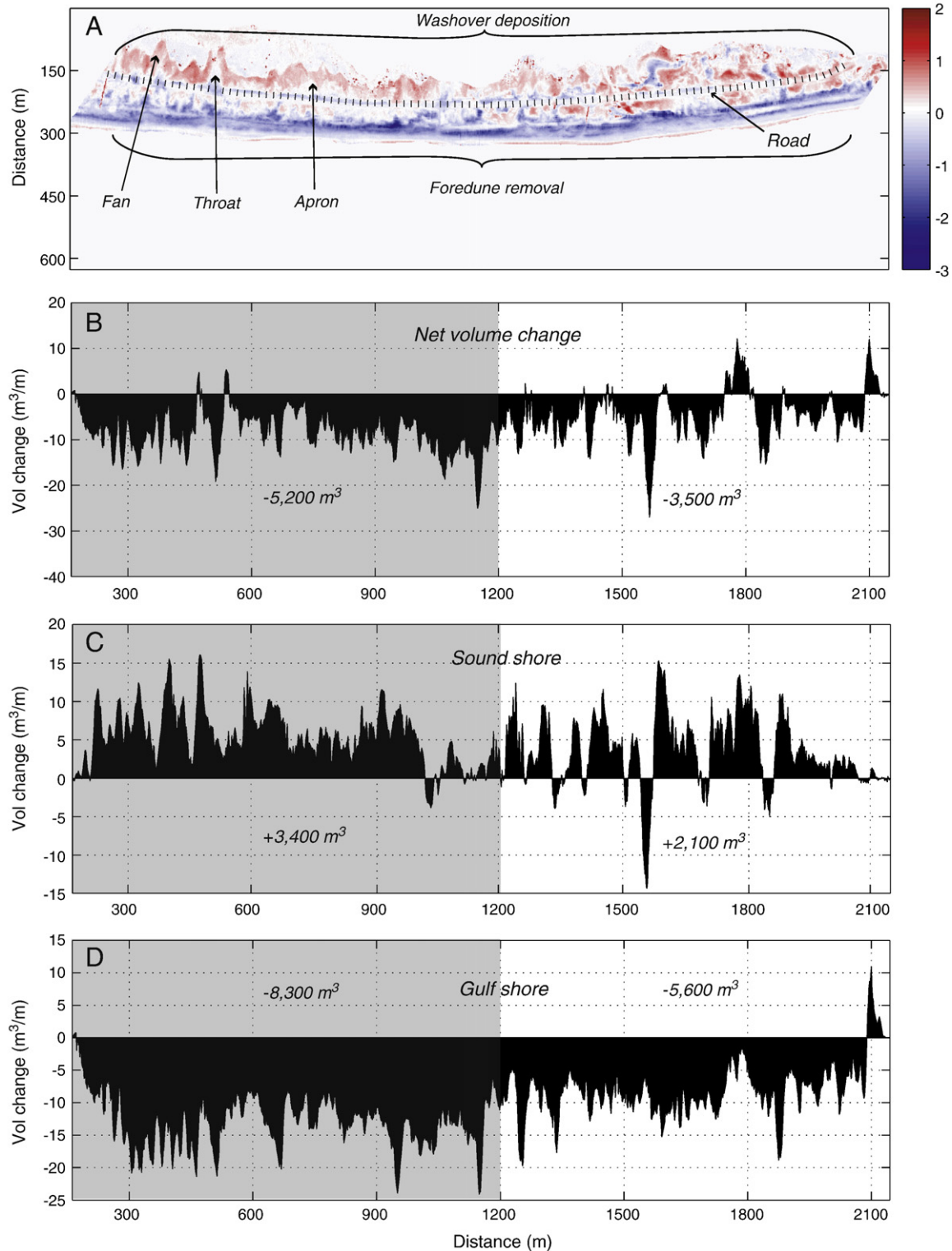


**Fig. 6.** Elevation change map (ECM) with calculated volume changes per unit width. Total volume changes in the study area differed depending upon the initial volume present and original foredune heights. The western half of the area experienced increased subaerial erosion (shaded gray) due to lower foredune elevations compared to the eastern half. Color bar in meters of elevation.

**Table 1**

Summary comparison of volume change variations along the western half (shaded gray) and eastern half of the DEM.

	West pre-volume	$\Delta V$	% of $V_{pre}$	East pre-volume	$\Delta V$	% of $V_{pre}$
Total	54,348	-5200	11	58,543	-3500	6
Gulf-shore	35,018	-8300	24	34,810	-5600	16
Sound-shore	17,091	3400	20	21,203	2100	10

Total refers to the combined gulf-shore and sound-shore sections. Pre-volume units in  $m^3$ ,  $\Delta V$  = volume change ( $m^3$  per m width of beach).

areas) indicate deposition. Numerically estimated volume changes to the study area (indicated by the swathed area in Fig. 1A) are shown in Fig. 6B–D. The net change in subaerial sediment volume, within the 2 km LiDAR section, was calculated to be on the order of  $-8700 m^3$  ( $-7 m^3/m$  of beach width) or 7% of the pre-storm volume above mean sea level (Fig. 6B). To gauge the sediment contribution from the foredunes and washover deposits to the net volume change, we categorized the DEM into four quadrants: eastern gulf-shore, eastern

sound-shore, western gulf-shore, and western sound-shore (the road served as the delineation between the gulf-shore and sound-shore sections). The gulf-shore section is characterized by sediment removal, while the sound-shore section is characterized by sediment deposition. Likewise, eastern half is characterized by relatively high and continuous foredunes, as opposed to the western half, which is characterized by lower, less continuous foredunes. Sediment loss to the total gulf-shore section was estimated at  $-13,900 m^3$ , about 60% of which occurred along the western quadrant where the foredunes were lowest (shaded gray in Fig. 6D). The total sound-shore experienced net deposition of  $5500 m^3$  with only a few locations that experienced any significant sediment loss. The western sound-shore quadrant also received a greater amount of sediment ( $3400 m^3$ ), accounting for about 61% of the total amount deposited (gray highlighted in Fig. 6C). Thus, across the subaerial portion of the barrier the western gulf-shore experienced more erosion while the western sound-shore received more sediment, despite the pre-storm volume of the western half ( $54,348 m^3$ ) being less compared to its eastern counterpart ( $58,543 m^3$ ). In other words, the western half lost a greater percentage of its pre-storm volume in the gulf-shore (24%)

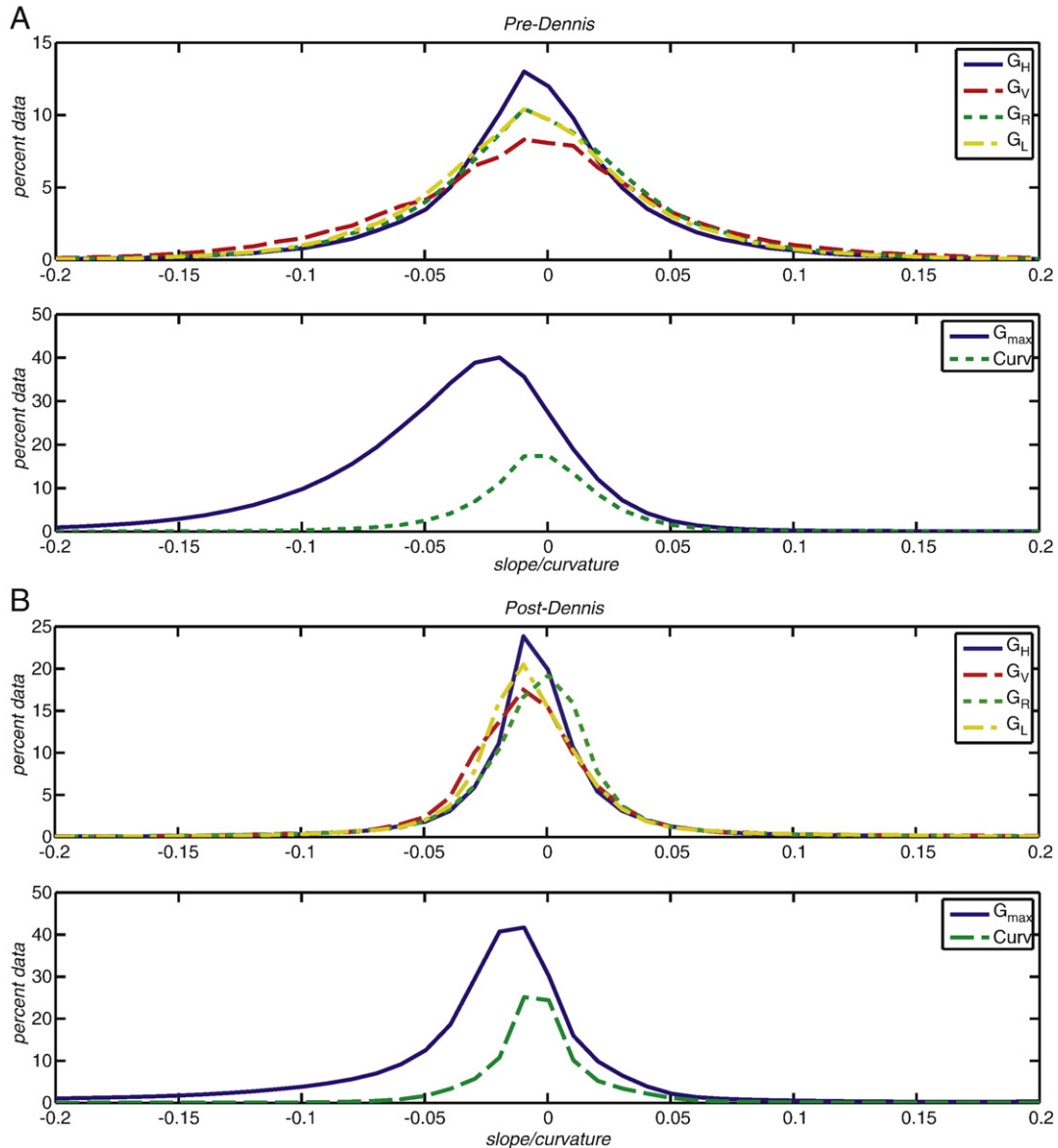


**Fig. 7.** Gradient (A) and maximum gradient/curvature (B) distributions calculated from pre-Dennis DEM.  $G_H$  = alongshore,  $G_V$  = cross-shore,  $G_R$  and  $G_L$  = right and left oblique directions,  $G_{max}$  = maximum gradient, Curv = curvature; see text for details.



**Table 2**

Table of the mean, standard deviation, skewness, and kurtosis for calculated gradients from the DEM.

	Aspect	Mean	Stdev	Skew	Kurt	
Gulf half	Pre	H	0.001	0.059	2.059	26.928
		V	-0.003	0.106	2.769	16.853
		RO	0.011	0.063	-0.392	6.240
		LO	0.002	0.079	2.402	14.359
		Max	0.011	0.093	1.180	8.862
	Post	H	0.001	0.042	5.962	120.008
		V	0.000	0.081	6.059	47.385
		RO	0.009	0.031	1.936	35.247
		LO	0.000	0.059	5.437	45.870
		Max	-0.008	0.053	4.448	69.932
Sound half	Pre	H	0.003	0.057	2.265	24.383
		V	0.014	0.064	2.228	22.551
		RO	0.000	0.066	3.154	20.678
		LO	0.010	0.052	1.549	17.399
		Max	0.011	0.071	0.895	11.859
	Post	H	0.003	0.068	1.632	44.600
		V	0.012	0.073	2.562	39.721
		RO	0.002	0.068	2.499	25.835
		LO	0.009	0.059	1.883	30.841
		Max	0.008	0.083	1.115	32.115
Total	Pre	H	0.001	0.054	1.237	18.349
		V	0.001	0.072	1.173	12.371
		RO	0.002	0.055	-0.028	7.375
		LO	0.001	0.057	0.966	10.853
		Max	-0.001	0.081	0.716	8.000
	Post	H	0.001	0.052	1.880	69.076
		V	0.002	0.058	3.054	51.916
		RO	0.002	0.045	0.525	35.954
		LO	0.002	0.047	2.326	44.336
		Max	0.000	0.067	1.596	41.336
	Curv	0.000	0.032	-4.830	137.279	

Aspect refers to the directions in which the gradients were calculated: H = horizontal (alongshore), V = vertical (cross-shore), RO = right oblique, LO = left oblique; the maximum gradient in any direction for each DEM grid point is (Max), and the curvature is (Curv).

and gained a greater percentage of its pre-storm volume in the sound-shore (20%) as compared to the eastern quadrants (16% and 10%, respectively; see also Table 1). This implies that much of the sediment stored in the foredunes along the eastern half was lost offshore instead of being deposited as a washover fan or apron. Finally, the higher erosion in the western part of the study area can also be ascribed to the island orientation with respect to the incoming hurricane waves from southwest.

## 4.2. Topographic gradient and curvature analyses

Topographic gradient and curvature distributions for pre- and post-storm events are plotted in Fig. 7A–B. Each plot illustrates the distribution for each direction along which the gradients were calculated, and the distribution of maximum gradient and curvature for each point of the DEM matrix. Pre- and post-storm distributions were calculated for the total DEM (Fig. 7), sound-shore and gulf-shore sections; Table 2 summarizes the results. In this analysis, an area that displays morphological features (e.g. dunes and fans) should plot as a broad-shoudered distribution, whereas flat surfaces should be tightly distributed around zero. Fig. 7A shows the pre-storm topographic gradient distributions in which the cross-shore distribution ( $G_V$ ) is broader than the distribution in the alongshore direction ( $G_H$ ), due to the steeper slopes that are found on the lee and stoss sides of the foredune complex. This is reflected in the standard deviation values in Table 2, which are higher for cross-shore gradients in the gulf side. As expected, pre-storm gradient distributions are much broader than the post-storm distributions, and this is numerically verified by consistent increases in kurtosis as shown in Table 2. The calculations also indicate that most of the pre-storm landforms, defined herein as non-flat areas, are distributed in the gulf-shore, whereas most of the post-storm landforms are located in the sound-shore. In fact the standard deviation of the topographic gradients in the gulf-shore decreases after the storm, whereas it increases in the sound-shore (see Table 2). This is because before the storm the gulf-shore was characterized by steep foredunes while only gentle secondary dunes were present in the sound-shore part of the island. The storm surge eroded the foredune complex flattening the gulf-shore topography and depositing sediments in the sound-shore in washover fans and aprons. These depositional features terminate with steep slopes (near the angle of repose for sand) and are responsible for the statistical change in topographic gradients in the sound-shore area.

Most of the distributions are left-tailed (having positive skewness) meaning the majority of gradients are distributed shoreward (for the vertical, or cross-shore, distribution calculated as negative gradients) than landward (positive gradients in the cross-shore direction). Within the gulf-shore, skewness in the cross-shore direction becomes more positive following the storm, and is probably caused by an increase in shoreward-sloping surfaces subsequent to the removal of the foredune complex (see Fig. 5A–F).

## 4.3. Recovery of secondary dunes

Topographic variations along five transects (Fig. 1) spanning one year and a half were analyzed to determine the rate of recovery of secondary dunes.

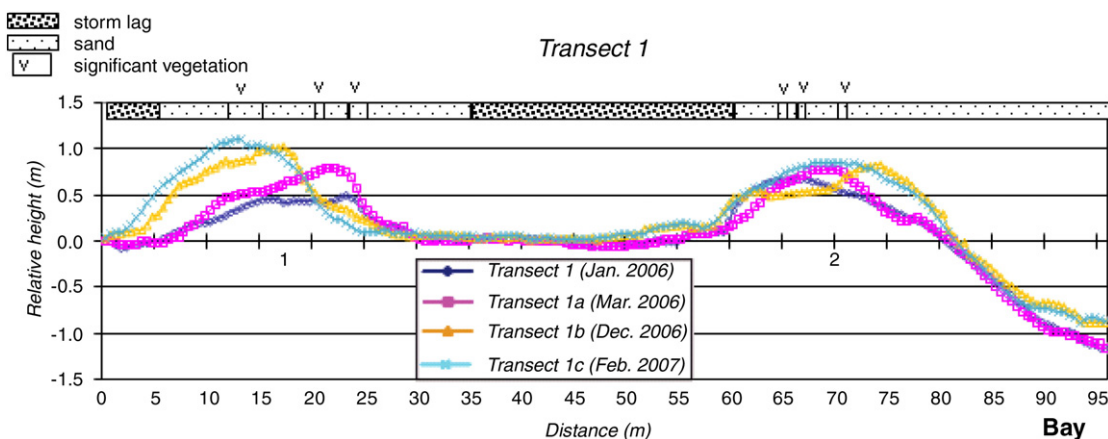


**Fig. 8.** Transect 1 profiles (Jan. 2006–Feb. 2007). Dunes 1 and 2 had gained 65 and 16 cm of height, respectively, and this area accumulated sediment on average of  $1.4 \text{ m}^3/\text{m}$  per month ( $16 \text{ m}^3/\text{m}$  net accumulation) throughout the duration of measurements. Note the lack of erosion or deposition in areas containing storm lag.

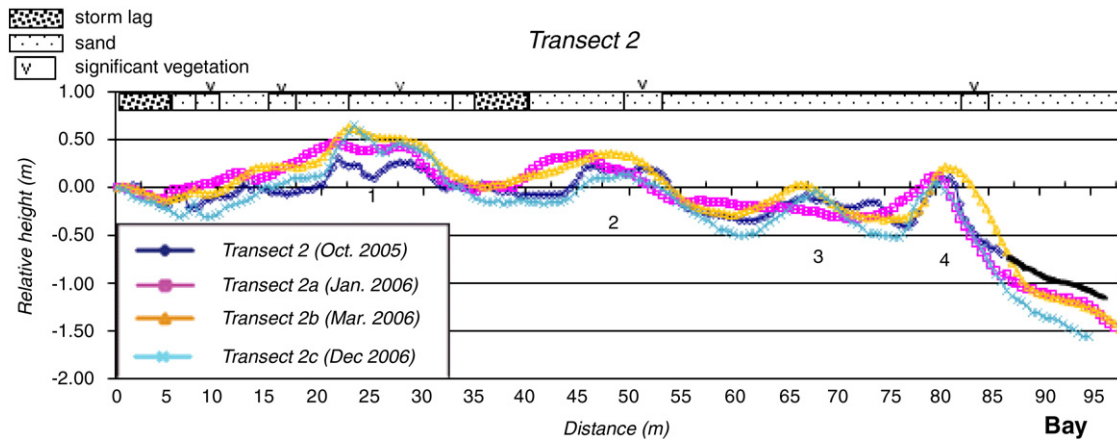


**Fig. 9.** Transect 2 profiles (Oct. 2005–Dec. 2006). Dunes 1, 2, and 4 occur in the vicinity of vegetation and are the most stable. Dune 1 was the least negatively affected during high wind events, which caused translations in dunes 2 and 4, and deflation of dune 3. Net erosion was  $-2.3 \text{ m}^3/\text{m}$ ; however, dune 1 accumulated sediment at an average rate of  $0.3 \text{ m}^3/\text{m}$  per month (between 20–35 m). Most of the net erosion was due to water-driven deflation of the washover fan (85–95 m). Black solid line indicates extrapolated surface.

4.3.1. *Transect 1*

Along the transect there are two prominent dunes, both vegetated (Fig. 8). The maximum height of the dunes was 0.45 and 0.69 m in January 2006; by February 2007, they had grown to heights of 1.10 and 0.85 m, respectively.

Each profile and subsequent volume change calculation shows consistent vertical accretion of dunes between measurements. Most of the accumulation,  $+12.0 \text{ m}^3/\text{m}$ , occurred between March and December, 2006; the total volume change for the year was  $+16.4 \text{ m}^3/\text{m}$ . Between the two dunes there was a significant amount of storm lag deposit on which no sediment accumulation or erosion occurred. Dune growth during the year is probably attributable to strong and persistent winds measured in excess of 9 m/s (20 mph) from ENE, and high frequency winds from the SE to SW in excess of 4 m/s (10 mph). Shifting of dune 1 is likely a result of high frequency northerly winds greater than 6.5 m/s (15 mph) during the month of November 2006 (see Fig. 2). The average sediment accumulation rate for the area was approximately  $1.4 \text{ m}^3/\text{m}$  per month.

4.3.2. *Transect 2*

High wind events measured between March 2006 and October 2006 resulted in net sediment loss along transect 2 (Fig. 9). Because of the long duration between measurements, it is difficult to assess which specific wind events caused the erosion, though it was probably the result of north winds  $> 10 \text{ m/s}$  that occurred between September

24th and October 26th 2006 (see Fig. 2). Despite this loss, the region corresponding to the first dune (15–30 m from the start of the transect) accumulated sediment. Overall, the dune field around transect 2 eroded at an average rate of  $-0.2 \text{ m}^3/\text{m}$  per month, most of which is accounted for between March and October 2006. Despite the net erosion, the first dune (at 15–30 m) accumulated an average of  $0.3 \text{ m}^3/\text{m}$  per month of sediment and gained about 36 cm in height over the duration of measurements, while dune 2 increased by 20 cm. Dune stability was also shown to be affected by the extent of vegetation. For instance, the second dune seemed to be more susceptible to translations where vegetation density was estimated to be relatively low ( $< 15\text{--}30\%$  cover). Where there was no vegetation, dune accretion or erosion was erratic, as shown in dune 3 (Fig. 9). Where vegetation density was estimated to be relatively high ( $> 30\%$  cover), dunes were more likely to withstand strong wind events, as shown in dunes 1 and 4. Similar behaviors occurred along vegetated areas of other transects.

4.3.3. *Transect 3*

Transect 3 profiles were taken on a washover fan that was devoid of vegetation and essentially featureless (Fig. 10). Here, stabilized dunes were nonexistent and the morphologic behavior of the profiles was constantly changing and erratic. Moreover, the net local (meaning in the vicinity of the transect) losses in sediment were much higher than those of vegetated areas ( $-17.9 \text{ m}^3/\text{m}$  over a 1 year

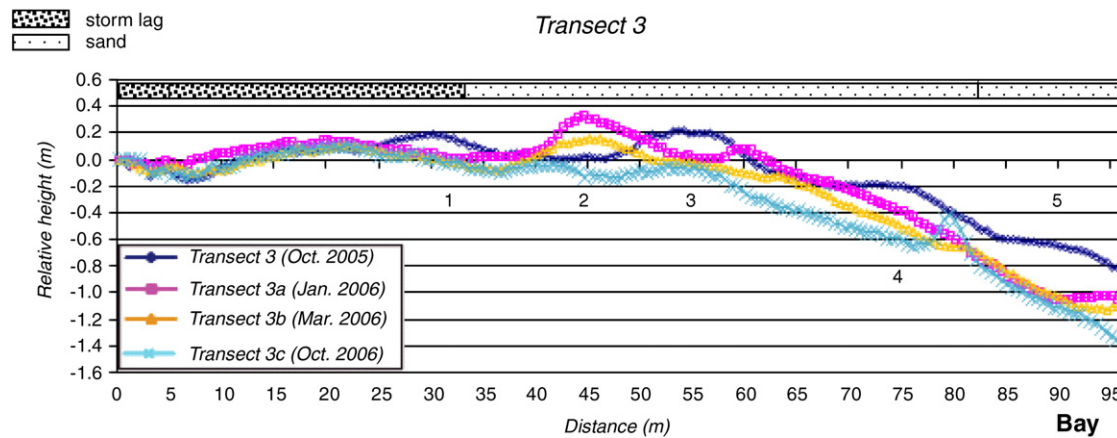


**Fig. 10.** Transect 3 profiles (Oct. 2005–Oct. 2006). Transect 3 was located on a washover throat and was severely scoured. As such, vegetation has difficulty establishing and the dunes present in the profiles are never stable. In fact, they are sand shadows created downwind from adjacent vegetation. Some of the net erosion,  $-17.9 \text{ m}^3/\text{m}$ , was due to water-driven deflation beyond 85 m where the terminating end of the washover deposit had reached the sound. The average erosion rate was  $-1.5 \text{ m}^3/\text{m}$  per month ( $-1.2 \text{ m}^3/\text{m}$  per month if including only the first 85 m). Again, note the lack of change in the storm lag region.

period). Due to lack of vegetation, this area eroded at an average rate of  $-1.5 \text{ m}^3/\text{m}$  per month, some of which (the last 25 m of the transect) was related to erosion by waves generated from St. George Sound. Not including the last 25 m, the overall average monthly erosion rate is still about  $-1.2 \text{ m}^3/\text{m}$ . Very little erosion or accumulation occurred in the first 20–25 m where storm lag deposits were pervasive.

#### 4.3.4. Transect 4

There were two prominent dunes along transect 1, near 10 m and 70 m from the beginning of the transect, the latter of which (shown as dune 2 in Fig. 11) changed very little over the study period. Dune 2 is a remnant dune that survived the overwash event, evidenced by a steep shore-facing scarp with exposed roots; it had remained at its original relative height of 1.5 m. Most of the sediment volume change occurred between 0–65 m. The total sediment volume change was about  $12 \text{ m}^3/\text{m}$  with an average rate of  $1.0 \text{ m}^3/\text{m}$  per month. The most noticeable changes were to the first dune, which increased its height by about 35 cm over the study period, and the progressive infilling in front of the scarp at the toe of the second dune.

#### 4.3.5. Transect 5

Seven profiles were acquired along transect 5 between May 2006 and February 2007 (Fig. 12). This transect, unlike transects 1–4, begins in the hummocky secondary dune environment and traverses shoreward 125 m into the backshore. The trend of the transect is nearly east–west and is therefore not shore-normal. There are four distinct physical settings along this transect: 1) 0–25 m, featureless sand and storm lag; 2) 25–60 m, prominent secondary dunes; 3) 60–100 m, anthropogenically vegetated backshore; and 4) >100 m, backshore and beach. The profiles along transect 5 showed relatively little change during the eight months between May 2006 and February 2007. Most of the measured change occurred beyond 85 m within the dynamic beach and backshore areas.

A net accumulation of sediment occurred between each measurement except June–July 2006 ( $-5.1 \text{ m}^3/\text{m}$ ) and October–December 2006 ( $-2.2 \text{ m}^3/\text{m}$ ). During these months, we measured short interval (60–230 min) wind events of greater than 6.5 m/s (15 mph) which were usually from the NNW, or offshore direction; this “loss” may occur locally, as sediment is redistributed and trapped by vegetation elsewhere rather than being lost to the system entirely.

The greatest sediment accumulation along transect 5 occurred between September and October, 2006. Three strong wind events exceeding 9 m/s (20 mph) with gusts reaching 12 m/s (26 mph) were recorded from the NE and ESE (shore-parallel and onshore, respec-

tively). These events probably supplied sediment from the beach to the backshore and subsequent dune field. The October storm is responsible for the ridge and runnel visible in the transect between 135–155 m. The piling of sediment that created the berm is responsible for much of the net sediment accumulation between September and October 2006; however, 5–10 cm of sediment had accumulated over most of the transect. Overall, the total sediment accumulation along transect 5 was  $10.8 \text{ m}^3/\text{m}$  with an average monthly accumulation rate of  $1.2 \text{ m}^3/\text{m}$  per month.

Excluding the beach and backshore (100–150 m), all measured accumulation occurred within vegetated areas. The region between 60–100 m originally began as non-vegetated sand with some storm debris. Sea oat seedlings were then planted uniformly by park service personnel as part of a dune restoration project. The seedlings were planted around June, 2007 and were about 10 cm in height with a density cover of about 30%, and by February 2008, they had grown to about 30 cm. This small amount of vegetation had a marked effect on sediment accumulation, increasing by nearly 40 cm (dune 4) over a six month period along the backshore at the vegetation boundary. Once sediment is transported across the boundary, further mobility is inhibited, which initiates dune building at the boundary.

## 5. Discussion

### 5.1. Sediment volume change

The total estimated subaerial volume of sediment removed following the hurricane was  $-8700 \text{ m}^3$ , of which ~60% occurred along the western half of the study area where foredunes were lowest. However, there was more sediment deposition in the western half of the sound-shore section than in the eastern half, despite lower foredunes and less initial sediment volume above mean sea level. This suggests that breaching and subsequent washover of the foredune complex along the western half occurred more rapidly than the eastern half. Thus, more sediment was translated landward as a result of waves and sheetflow toward the back-barrier. In contrast, the higher, continuous foredunes along the eastern half probably delayed the overwash event, so that wave activity only scoured the toe of the dunes, initially transporting larger volumes of sediment offshore as the storm surge rose. Once the combined storm surge and wave run-up exceeded the height of the foredunes, sediment began to move landward carried by the storm surge. This process accounts for the reduced net sediment loss and the extensive beach widening along the eastern half of the DEM. The remainder of sediment in the system is likely to have been stored offshore. The average net erosion along

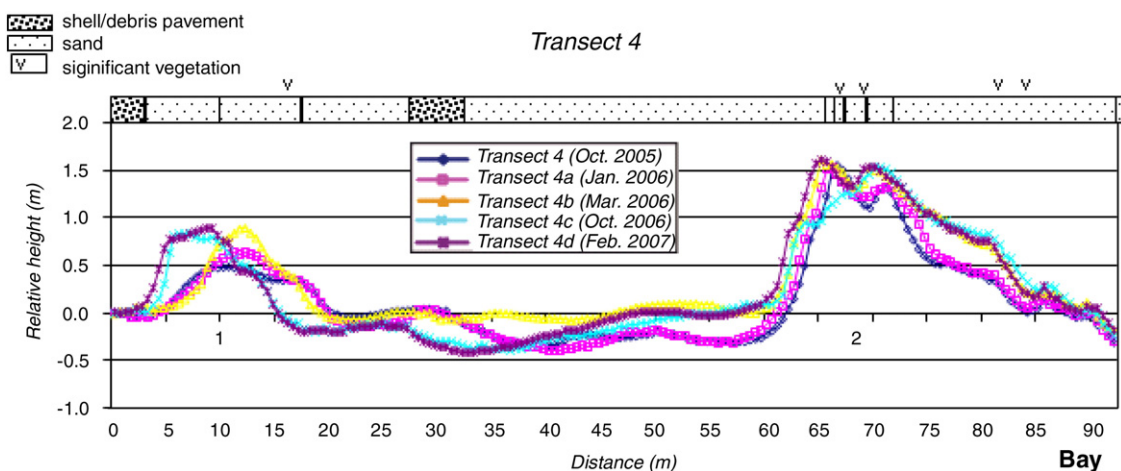


**Fig. 11.** Transect 4 profiles (Oct. 2005–Feb. 2007). Here, dune 2 is a remnant surviving dune evidenced by the shore-facing scarp. Dune 2 is heavily vegetated on the stoss side and remained stable throughout the study period. Note the progressive infilling of the scarp face. Dune 1 had increased its height by about 35 cm. The average sediment accumulation rate was  $1.0 \text{ m}^3/\text{m}$  per month ( $12 \text{ m}^3/\text{m}$  net accumulation).

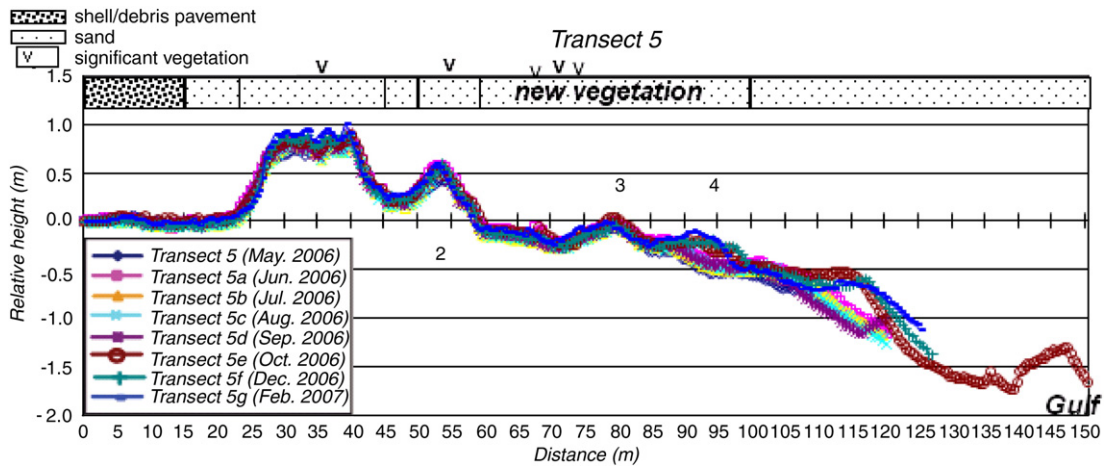


**Fig. 12.** Transect 5 profiles (May 2006–Feb. 2007). Vegetation was already well established (by natural dissemination) by May 2006, accounting for the noticed stability of the profiles between 0–60 m. Newly planted sea oats (June 2007) from 60–100 m caused significant accumulations of sediment, especially at the vegetation boundary (100 m), where wind speeds are great enough to transport sand from the beach face just landward of the vegetation boundary, but not much farther (see text for more details).

this 2 km segment of the park was estimated at  $-7 \text{ m}^3/\text{m}$  of beach width. This is similar to values reported by Leatherman (1976) which ranged from  $-1$  to  $-7.5 \text{ m}^3/\text{m}$  of beach width along a 30 m overwashed section of Assateague Island, Maryland caused by nor'easter storms. In contrast, Wang et al. (2006) reported a net sediment loss of  $-20 \text{ m}^3/\text{m}$  across a 550 m profile for a narrow section of the northwest Florida barrier chain at Beasley Park (80 km to eyewall), post-hurricane Ivan in 2004.

Recent studies on the effect of hurricane Ivan on Santa Rosa island showed that overwash events transported large volumes of sand from the nearshore foredune to the back-barrier area, producing fan and apron deposits. Overall the barrier island conserved mass, with the eroded volume approximately equal to the deposited one (Stone et al., 2005). A similar redistribution pattern is also valid for our study site in St. George Island after hurricane Dennis, although we compute a net sediment loss of  $8700 \text{ m}^3/\text{m}$ , equivalent to 7% of the total subaerial volume of the island. We therefore conclude that despite washover deposits are largely composed of sediments eroded from the foredune and shoreface, the island does not always conserve mass after a hurricane event, but a significant volume is lost to offshore areas and to the back-bay.

Our data analysis shows that foredune erosion was higher when the dune complex was lower and discontinuous. This is in accordance with the results of Houser et al. (2008a,b) and Houser and Hamilton (2009), who showed that areas with high foredunes and back-barrier dunes experience less overwash penetration. Houser and Hamilton (2009) further indicate that alongshore variation in recovery is related to island width, the amount of overwash penetration, and the presence of transverse ridges in the inner shelf.

Finally, since the topographic expression of the barrier was rendered nearly featureless after the storm, there was very little topographic gradient. This lack of steep surfaces is represented as a calculated topographic gradient distribution in which most of the values are centered relatively close to zero (no slope). As dunes build through time, it should be possible to see these changes reflected in a relatively broader distribution. For a given control area, these changes in distribution can be quantified by calculating the variance and the kurtosis, or peakedness, of the distributions. To obtain the most accurate results, the LiDAR datasets should match a set of bounding coordinates with respect to a chosen reference area, and using the same grid spacing and fill method (e.g., linear interpolation). We propose that this simple numerical analysis can be applied to rapidly estimate the “relative recovery state” of the barrier by comparing post-storm distributions of gradients to a pre-storm reference distribution (the post-storm dataset would be used as the reference

dataset in order to gauge recovery after storm impact). This type of analysis is intended to provide a gross view of the recovery and cannot account precisely for where the recovery is taking place.

It is important to note that several LiDAR datasets prior to a hurricane are, in reality, necessary to determine the natural, pre-storm topography and its variability in time. In fact dune fields are inherently dynamic and quickly respond to small variations in wind climate and vegetation cover, so that, even in absence of major storms, their topographic characteristics change in time. The diffusion of LiDAR altimetry will provide enough datasets in the future for a correct determination of the target natural topography for restoration projects.

### 5.2. Secondary dune recovery

Wang et al. (2006) indicated that initial post-storm recovery occurs on the order of a few months along the foreshore-slope and beach environments, while this study finds that significant growth of hummocky secondary dunes within the back-barrier may occur within 1 year providing sediment is supplied in the presence of vegetation; although, complete recovery may take longer especially if the recovery process is interrupted by subsequent storms (Stone et al., 2004).

Recovery of dunes in the back-barrier is facilitated by available sediment, wind, and vegetation. The lack of a foredune and significant vegetation across the study site following hurricane Dennis allowed for exchange of aeolian-driven sediments between the beach and the back-barrier. Sediments were probably supplied to the beach as a result of landward migration and subsequent welding of offshore bars onto the beach in the days following the storm (Morton et al., 1994; Aagaard et al., 2004; Houser and Greenwood, 2007). Onshore winds can then transport the sediment to secondary dune fields, while deflation of washover deposits provides a local sediment source during offshore and alongshore winds (Leatherman, 1979; Houser et al., 2008a). Areas of the back-barrier containing moderate amounts of vegetation consistently accreted sediment, while those without vegetation remained unchanged if in the presence of storm lag deposits, or otherwise behaved erratically as sediment is mobilized by wind. An armoring effect of storm lag deposits was noted by Houser et al. (2008a,b) to have a limiting effect on sediment transport across the beach face. This study also noted an armoring effect within the back-barrier; however, armoring by storm lag was not observed to limit sand transport. Instead, the only effect was to limit subaerial deflation noted by insignificant profile changes within these areas, as also noted by Leatherman and Zaremba (1987). Sediment transport across the beach face into the back-barrier should conceivably continue until the

development of a frontal dune system (with vegetation density >30%), which will significantly reduce the sand transport rate on the immediate landward side of the dune. If a barrier contains pockets of vegetation (as in our case), then areas without vegetation act as a local sediment source to the dunes from any prominent wind direction and strength sufficient to mobilize the sand (vegetation is efficient at trapping sand from any direction). As such, after a large storm has deposited sediment in the back-barrier, the recovery of the secondary dunes depends primarily on the presence of vegetation and the ability of wind to redistribute the sediment throughout the year. Indeed if the recovery rates are initially high in the first few months to 1 year after overwash, then perhaps newly expanding plant colonies force attenuating sediment fluxes across the barrier through time. Therefore, from a coastal management perspective, it may be more useful to allow sufficient time for beach recovery and welding of offshore bars before revegetation projects are initiated. Once foredunes recover, the back-barrier should become a sediment limited system, relying primarily on locally derived sediments.

## 6. Conclusions

The following set of conclusions is derived by our geomorphological analysis of storm surge effects on St. George Island and its related recovery:

1. At locations where the foredune system was lower and discontinuous the overwash event flattened the foredune system moving the eroded sand to the back-barrier forming washover fans and aprons. Where the foredunes were high and well developed less sediment was moved to the back-barrier and a larger fraction of eroded material was transported offshore.
2. Statistical analysis of topographic gradients and curvatures shows that the gulf-shore part of the island became more flat after the storm whereas the sound-shore area became slightly steeper due to washover deposits. Generally, topographic gradients were reduced with a narrower distribution. Distribution of topographic attributes can be used to determine the stage of recovery of barrier islands after storm events.
3. The recovery of secondary dunes was not immediate but still ongoing one year and a half after the hurricane. Already existing dunes accreted whereas flat areas (e.g. overwash fans and aprons) were subjected to erratic variations in topography without the establishment of new dunes. The secondary dunes recovered at an average rate of 3–4 cm per month in the presence of vegetation, although average monthly volume changes varied from  $-1.5$  to  $1.2$  m<sup>3</sup>/m, and total volume changes varied from  $-17.9$  to  $16.4$  m<sup>3</sup>/m across the transects for the duration of the study.
4. The presence of vegetation stabilized dunes, favoring accretion and reducing dune migration. On the contrary, storm lag deposits composed of shells and debris prevented vegetation encroachment and dune formation. Areas with lag deposits remained flat with no topographic change during the study period, bypassing all sediments to nearby areas.

## Acknowledgments

This research has been partly funded by the Petroleum Research Fund Award No. 42633-G8, the Office of Naval Research, Award No. N00014-05-1-0071. We thank the reviewers whose comments and criticisms greatly benefitted the final version of this manuscript.

## References

Aagaard, T., Davidson-Arnott, R.G.D., Greenwood, B., Nielsen, J., 2004. Sediment supply from shoreface to dunes—linking sediment transport measurements and long term morphological evolution. *Geomorphology* 60, 205–224.

- Andrews, B.D., Gares, P.A., Colby, J.D., 2002. Techniques for GIS modeling of coastal dunes. *Geomorphology* 48, 289–308.
- Arens, S.M., 1996. Patterns of sand transport on vegetated dunes. *Geomorphology* 17, 339–350.
- Beaches and Shores Resource Center, 1983. Coastal construction control line review and study for Franklin County. Florida, Florida State University. 83 pp.
- Brock, J.C., Wright, W., Sallenger, A.H., Krabill, W.B., Swift, R.N., 2002. Basis and methods of NASA airborne topographic mapper lidar surveys for coastal studies. *Journal of Coastal Research* 18, 1–13.
- Buckley, R., 1987. The effect of sparse vegetation cover on the transport of dune sand by wind. *Nature* 325 (6103), 426–428.
- Claudino-Sales, V., Wang, P., Horwitz, M.H., 1987. Factors controlling the survival of coastal dunes during multiple hurricane impacts in 2004 and 2005: Santa Rosa barrier island, Florida. *Geomorphology* 95, 295–315.
- Dingler, J.R., Reiss, T.E., 1990. Cold-front driven storm erosion and overwash in the central part of the Isles-Dernieres, a Louisiana barrier-island arc. *Marine Geology* 91, 195–206.
- Donnelly, C., Kraus, N., Larson, M., 2006. State of knowledge on measurement and modeling of coastal overwash. *Journal of Coastal Research* 15, 965–991.
- Hesp, P.A., 1989. A review of biological and geomorphological processes involved in the initiation and development of incipient foredunes. In: Gimingham, C.H., Ritchie, W., Willets, B.B., Willis, A.J. (Eds.), *Coastal Sand Dunes*. Proceedings of the Royal Society of Edinburgh, vol. 96B. Roy. Soc. Edinb, Edinburgh, pp. 181–202.
- Hesp, P.A., Davidson-Arnott, R., Walker, I.J., Ollerhead, J., 2005. Flow dynamics over a foredune at Prince Edward Island, Canada. *Geomorphology* 65, 71–84.
- Houser, C., Greenwood, B., 2007. Onshore migration of a swash bar during a storm. *Journal of Coastal Research* 23, 1–14.
- Houser, C., Hamilton, S., 2009. Sensitivity of post-hurricane beach and dune recovery to event frequency. *Earth Surface Processes and Landforms* 34, 613–628.
- Houser, C., Hobbs, C., Saari, B., 2008a. Posthurricane airflow and sediment transport over a recovering dune. *Journal of Coastal Research* 24, 944–953.
- Houser, C., Hapke, C., Hamilton, S., 2008b. Controls on coastal dune morphology, shoreline erosion and barrier island response to extreme storms. *Geomorphology* 100, 223–240.
- Irish, J.L., White, T.E., 1998. Coastal engineering applications of high-resolution lidar bathymetry. *Coastal Engineering* 35, 47–71.
- Leatherman, S.P., 1976. Quantification of Overwash Processes. Thesis, University of Virginia, 245 pp.
- Leatherman, S.P., 1979. Barrier dune systems: a reassessment. *Sedimentary Geology* 24, 1–16.
- Leatherman, S.P., Zaremba, R.E., 1987. Overwash and aeolian processes on a U.S. northeast coast barrier. *Sedimentary Geology* 52, 183–206.
- Morton, R.A., Sallenger, A.H., 2003. Morphological impacts of extreme storms on sandy beaches and barriers. *Journal of Coastal Research* 19, 560–573.
- Morton, R.A., Paine, J.G., Gibeau, J.C., 1994. Stages and duration of post-storm beach recovery, southeastern Texas coast, U.S.A. *Journal of Coastal Research* 10, 884–908.
- Robertson, W., Zhang, K., Whitman, D., 2007. Hurricane-induced beach change derived from airborne laser measurements near Panama City, Florida. *Marine Geology* 237, 191–205.
- Sallenger, A.H., Krabill, W., Brock, J., Swift, R., Jansen, M., Manizade, S., Richmond, B., Hampton, M., Eslinger, D., 1999. Airborne laser study quantifies El Niño-induced coastal change. *EOS. Trans. Am. Geophysical Union* 80 (89), 92–93.
- Sallenger, A.H., 2000. Storm impact scale of barrier islands. *Journal of Coastal Research* 16, 890–895.
- Sallenger, A., Stockdon, H., Fauver, L., Hansen, M., Thompson, D., Wright, C.W., Lillycrop, J., 2006. Hurricanes 2004: an overview of their characteristics and coastal change. *Estuaries and Coasts* 29, 880–888.
- Saye, S.E., van der Wal, D., Pye, K., Blott, S.J., 2005. Beach–dune morphological relationships and erosion/accretion: an investigation at five sites in England and Wales using LIDAR data. *Geomorphology* 72, 128–155.
- Snyder, R.A., Boss, C.L., 2002. Recovery and stability in barrier island plant communities. *Journal of Coastal Research* 18, 530–536.
- Stallins, J.A., 2001. Dune plant species diversity and function in two barrier island biogeomorphic systems. *Plant Ecology* 165, 183–196.
- Stone, G.W., Liu, B., Pepper, D.A., Wang, P., 2004. The importance of extratropical and tropical cyclones on the short-term evolution of barrier islands along the Northern Gulf of Mexico, USA. *Marine Geology* 210, 63–78.
- Stone, G.W., Walker, N.D., Hsu, S.A., Babin, A., Liu, B., Keim, D., Teague, W., Mitchell, D., Leben, R., 2005. Hurricane Ivan's impact along the Northern Gulf of Mexico. *EOS. Transactions of the American Geophysical Union* 86, 497–508.
- van der Wal, D., 1996. The development of a Digital Terrain Model for the geomorphological engineering of the rolling foredune of Terschelling, The Netherlands. *Journal of Coastal Conservation* 2, 55–62.
- Wang, P., Kirby, J.H., Haber, J.D., Horwitz, M.H., Knorr, P.O., Krock, J.R., 2006. Morphological and sedimentological impacts of Hurricane Ivan and immediate poststorm beach recovery along the northwestern Florida barrier-island coasts. *Journal of Coastal Research* 22, 1382–1402.
- Woodhouse Jr., W.W., Seneca, E.D., Cooper, A.W., 1968. Use of sea oats for dune stabilization in the southeast. *Shore and Beach* 36, 15–21.